Journal of
Applied Crystallography

ISSN 0021-8898

Received 18 August 2008
Accepted 12 April 2009

Determination of the degree of preferred orientation within the March–Dollase approach

Emil Zolotoyabko

Department of Materials Engineering, Technion – Israel Institute of Technology, Haifa 32000, Israel.
Correspondence e-mail: zloto@tx.technion.ac.il

An analytic expression has been derived connecting the degree of preferred orientation in a polycrystalline material to the March parameter. The latter defines the spread of angular distribution of crystallite inclinations in the March–Dollase approach [March (1932). *Z. Kristallogr.* **81**, 285–297; Dollase (1986). *J. Appl. Cryst.* **19**, 267–272]. In turn, the March parameter can be extracted from experimental data using either the Rietveld refinement of the entire diffraction pattern or the measurement of two diffraction intensities originating in the selected crystallographic planes. Working examples taken with two different types of samples are presented.

1. Introduction

Practically all polycrystalline materials reveal some degree of preferred orientation of crystallites, owing to the forces evolving between them during crystal growth and material processing. For this reason, the measurement of preferred orientation (texture) is of great importance because in this way essential information on material characteristics can be obtained. Therefore, the development of fast and reliable methods to characterize quantitatively the preferred orientation and its modification under processing is highly desirable. However, despite intensive effort there is still a lack of fast well established techniques that would allow comparison of the texture of materials using a single parameter or a few of them.

Crystallographic texture is characterized by electron and X-ray diffraction methods. For electron diffraction, a specific mode of scanning electron microscopy is used, namely electron backscatter diffraction (EBSD) (see *e.g.* Adams *et al.*, 1993). In this mode, a specific diffraction pattern (Kikuchi lines) is registered from an individual grain by means of a CCD camera, and this is then converted to the grain orientation with respect to the sample surface. By taking diffraction patterns from a number of grains, the partial orientation distribution function (ODF) (limited by grain quantity) can be reconstructed. The EBSD method works well in a thin layer beneath the sample surface that is also restricted laterally on a scale in the 100 μm range.

Texture in deeper layers and averaged over much larger sample areas is traditionally examined by the X-ray diffraction methods, although nowadays, because of progress in synchrotron micro-diffraction techniques, it is also possible to follow the orientation of individual micrometre-sized grains and their transformations using X-rays (Poulsen, 2004).

There are several approaches for solving the texture problem with laboratory X-ray diffraction systems. The classical technique is based on the measurement of pole figures (Bunge, 1982). For this purpose, a conventional $\theta/2\theta$ diffractometer is used, equipped with a one-dimensional (slit) detector and a special texture attachment. The latter provides sample rotation by changing the tilt angle χ and azimuthal (in the plane of the sample) angle φ. Practically, one measures the diffraction intensity of a fixed reflection (fixed angle 2θ) as a function of χ and φ (pole figure). A pole figure (after appropriate instrumental corrections) shows the angular (χ, φ) distribution of the reciprocal lattice vector $\mathbf{h} = (hkl)$, which is normal to the chosen crystallographic plane. In turn, an inverse pole figure reflects the relative quantities of crystallites in which vectors $\mathbf{h}$ are nearly parallel to the sample direction z.

A more general approach, developed by Roe (1965) and Bunge & Haessner (1968), provides the complete ODF, which is defined as the relative volume of crystallites having orientations between $\mathbf{g}$ and $\mathbf{g} + d\mathbf{g}$ in the coordinate system attached to the main directions of the sample. The ODF brings comprehensive information on the preferred orientation and, in principle, can be extracted from a number of measured pole figures. This can be done, for example, by using a generalized spherical harmonic description (see *e.g.* Ahtee *et al.*, 1989; Popa, 1992; Järvinen, 1993; Von Dreele, 1997; Sitepu *et al.*, 2005) or by the Williams–Imhof–Matthies–Vinel (WIMV) method (see *e.g.* Matthies & Vinel, 1982; Lutterotti *et al.*, 1997; Matthies *et al.*, 1997). However, the ODF approach is rather time consuming because of the large amount of data which must be collected and processed.

An essential technical step forward was the use of two-dimensional detectors for texture examination (Smith & Ortega, 1993). A two-dimensional detector allows the capture of a considerable part of the diffraction cone (instead of only the small region available with a one-dimensional detector) and thus drastically increases the amount of information obtained during an individual measurement. By using two-dimensional detectors it is also possible, in some cases, to

eliminate the sample tilt in texture measurements (Kurtz *et al.*, 2001), which significantly reduces the data acquisition time. However, as has already been mentioned, all these developments fail to provide a simple algorithm that allows the quantitative description of the degree η of the preferred orientation ($0 \leq \eta < 100\%$) of the sample and its change under processing using a very limited set of parameters.

In this paper, we attempt to fill this gap in the framework of the March–Dollase approach (Dollase, 1986; Čapková *et al.*, 1993; Howard & Kisi, 2000). The latter uses the analytical weight function – the March function (March, 1932), which depends on a single parameter (March parameter, $0 < r \leq 1$) – in order to describe the preferred orientation of the investigated sample. It is worth emphasizing that, having originally been developed for uniaxial texture (where the weight function does not depend on the azimuthal angle φ), this correction can be successfully used in the Rietveld refinement of different materials (see *e.g.* Young, 1993, and references therein) and is now included in many currently available refinement packages, such as *GSAS* (Larson & Von Dreele, 1986). Moreover, the March–Dollase approach can be applied to describe quantitatively a strong preferred orientation, which causes the best part of the diffraction lines to vanish. In this case, Rietveld refinement is useless, but the March parameter can still be extracted from the measurement of two diffraction intensities originating in the selected crystallographic planes (see *e.g.* Zamir *et al.*, 2000; Zolotoyabko & Quintana, 2002*a*). These considerations show the great potential of the March–Dollase method.

At the same time, there are a very limited number of papers focused on preferred orientation itself and its modification in specific materials (see *e.g.* Deyu *et al.*, 1990; Leventouri, 1997; Zamir *et al.*, 2000; Zolotoyabko & Quintana, 2002*a*, Sitepu *et al.*, 2005). In all these papers, the March parameter r is extracted, whose physical meaning and link to the degree of preferred orientation is not very straightforward. It is believed that the degree of preferred orientation is $\eta = 100\%(1 - r)$, although this statement, to the best of our knowledge, has never been justified. Seemingly, it is based on the obvious facts that $\eta = 0$ for $r = 1$ (random powder) and η tends to 100% in the limit of $r = 0$ (perfect uniaxial preferred orientation), as well as on an intuitive assumption that the degree of preferred orientation is linearly related to the March parameter r in between.

Below, we develop an analytical procedure that offers a firm relationship between the degree of preferred orientation η and the March parameter r extracted from diffraction measurements. The resulting equation shows that the dependence $\eta(r)$ is not linear, although it provides the correct values of $\eta(0) = 100\%$ and $\eta(1) = 0$ at the boundaries of the r range.

2. Interrelation between the degree of preferred orientation and the March parameter

In the March–Dollase approach, the weight function $W(\alpha)$ is introduced to describe the fraction of crystallites in which the vectors of the reciprocal lattice **h** are parallel to the normal to the sample surface **n**, this being also the direction of the preferred orientation **H** (Dollase, 1986):

$$W(\alpha) = \left(r^2 \cos^2\alpha + \frac{1}{r}\sin^2\alpha\right)^{-3/2}. \quad (1)$$

The angle α in equation (1) is between the vectors **h** and **H** in a single crystal. The March parameter, $0 < r \leq 1$, determines the shape of the function $W(\alpha)$ and, respectively, the strength of the preferred orientation. At $r = 1$ (random powder), $W(\alpha) = 1$ and does not depend on α. At $r \rightarrow 0$ (perfect uniaxial preferred orientation), $W(\alpha)$ transforms to a delta function, $\delta(0)$. At intermediate r values, $0 < r < 1$, the $W(\alpha)$ function has a maximum at $\alpha = 0$ which grows rapidly as $W(0) = r^{-3}$ when the r value diminishes to zero (see Fig. 1). We stress that the same function in equation (1) describes the distribution of crystallites in which the vector of the reciprocal lattice **H** is inclined by an angle α with respect to the normal **n** to the surface of the sample (Dollase, 1986). Thus, the function $W(\alpha)$ should be normalized,

$$\int_0^{\pi/2} M(\alpha)\sin\alpha\,\mathrm{d}\alpha = 1, \quad (2)$$

reflecting the finite total number of crystallites with all possible inclinations of vector **H** with respect to vector **n**. This important point is directly proved below.

The natural way of defining the degree of preferred orientation is to connect it somehow to the fraction of crystallites $P(\alpha_0)$ having the inclination angle α in the range $0 \leq \alpha \leq \alpha_0$. The choice of characteristic angle α_0 will be discussed later. So, based on equation (1), the $P(\alpha_0)$ value can be expressed as

$$P(\alpha_0) = \int_0^{\alpha_0} \left(r^2 \cos^2\alpha + \frac{1}{r}\sin^2\alpha\right)^{-3/2} \sin\alpha\,\mathrm{d}\alpha. \quad (3)$$

Using the replacement $\cos\alpha = t$, the integral of equation (3) transforms into

$$P(\alpha_0) = r^{3/2} \int_{t_1}^{t_2} \mathrm{d}t\left[1 - (1 - r^3)t^2\right]^{-3/2}. \quad (4)$$

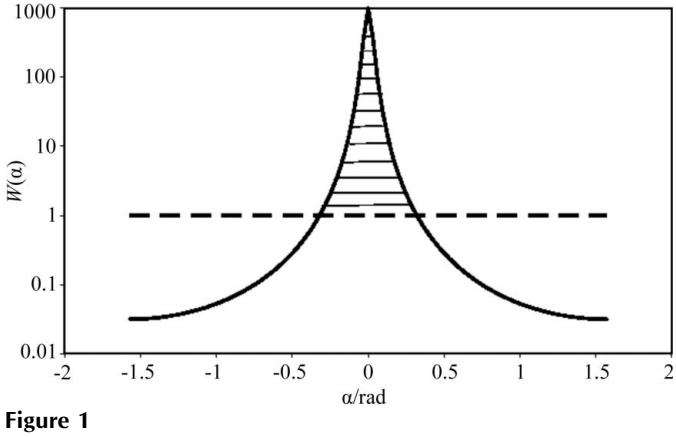

Figure 1
The March function $W(\alpha)$, calculated for $r = 0.1$ (solid line). The excess above the value for a random powder [$W(\alpha) = 1$; dashed line] is hatched.

A second replacement, $t = (1 - r^3)^{-1/2} \sin x$, yields a tabulated integral

$$P(\alpha_0) = \left[\frac{r^3}{(1 - r^3)}\right]^{1/2} \int_{x_1}^{x_2} \frac{dx}{\cos^2 x} = \left[\frac{r^3}{(1 - r^3)}\right]^{1/2} (\tan x_2 - \tan x_1). \quad (5)$$

Finally, using the reverse replacement $x = \arcsin[(1 - r^3)^{1/2} \cos\alpha]$, one obtains

$$P(\alpha_0) = \left[\frac{r^3}{(1 - r^3)}\right]^{1/2} \tan\left\{\arcsin\left[\left(1 - r^3\right)^{1/2} \cos\alpha\right]\right\}_{\alpha_0}^{0} = 1 - \xi \quad (6)$$

with

$$\xi = \left(1 + \frac{\tan^2 \alpha_0}{r^3}\right)^{-1/2}. \quad (7)$$

Note that if $\alpha_0 = \pi/2$, then $\xi = 0$ and $P = 1$, which justifies the normalization condition of equation (2). For a random powder ($r = 1$), equation (7) transforms into

$$\xi_p = \cos\alpha_0. \quad (8)$$

The degree of preferred orientation η is the excess of the $P(\alpha_0)$ value in a sample with $r \neq 1$ compared with a random powder, *i.e.*

$$\eta = 100\%\left[(1 - \xi) - (1 - \xi_p)\right] = 100\%\left(\xi_p - \xi\right) = 100\%\left[\cos\alpha_0 - \left(1 + \frac{\tan^2 \alpha_0}{r^3}\right)^{-1/2}\right]. \quad (9)$$

Obviously, the magnitude of η depends on the α_0 value. For example, $\eta = 0$ at $\alpha_0 = 0$. Therefore, we must allow the inclination angle α to be within some reasonable angular interval. We propose to restrict the latter to the point where the $W(\alpha)$ function is equal to its value for a random powder (see Fig. 1), *i.e.*

$$W(\alpha_0) = \left(r^2 \cos^2 \alpha_0 + \frac{1}{r} \sin^2 \alpha_0\right)^{-3/2} = 1. \quad (10)$$

Solving equation (10) for $r \neq 1$ yields

$$\cos\alpha_0 = \left(\frac{1 - r}{1 - r^3}\right)^{1/2}. \quad (11)$$

Finally, substituting equation (11) into equation (9) yields

$$\eta = 100\%\left[\frac{(1 - r)^3}{1 - r^3}\right]^{1/2}. \quad (12)$$

Equation (12) can be introduced into computer programs utilizing refinement of the March parameter r within the Rietveld routine in order to obtain the degree of the preferred orientation η. The magnitude of η as a function of r is plotted in Fig. 2. As expected, η tends to zero when r tends to 1. Defining $r = 1 - \varepsilon$, one obtains the asymptotic $\eta \simeq 100\%\ (\varepsilon/3^{1/2})$. At the other extreme, $r << 1$, the η value tends to 100% as $\eta \simeq 100\%\,[1 - (3/2)r]$. Equation (12) provides significantly different η values compared with the linear function $\eta_l = 100\%\ (1 - r)$, also plotted for comparison in Fig. 2. For example, at $r = 0.5$, $\eta_l = 50\%$ while $\eta = 37.8\%$.

Note that, formally, the approach described by equations (3)–(12) is developed for the pole in the weight function of equation (1) located at $\alpha = 0$ [integration between 0 and α_0 in equation (3)]. However, it is easy to show that exactly the same final equation (12) remains valid for the pole in the weight function of equation (1) located at $\alpha = \pi/2$ [integration between $\pi/2$ and $\pi/2 + \alpha_0$ in equation (3)]. As is known, this case corresponds to the March parameter ranging between 1 and ∞. This is standard, for example, for neutron diffraction measurements in transmission mode (see *e.g.* Sitepu *et al.*, 2001). Therefore, the final equation (12) can equally be used in both situations, *i.e.* $r \leq 1$ and $r \geq 1$.

3. Working examples

In practical terms, the degree of preferred orientation η in the framework of the March–Dollase approach can be determined in two different ways. If the effect of preferred orientation is weak, the best solution is given by applying the Rietveld refinement procedure to the whole diffraction pattern, extracting the March parameter r and determining the η value *via* equation (12). In the case of strong preferred orientation, many of the diffraction lines are drastically suppressed and application of Rietveld refinement becomes complicated. In this situation, the best way is to measure the intensities of two reflections, $\mathbf{H}(HKL)$ and $\mathbf{h}(hkl)$, one of them ($\mathbf{H}$) being that of the preferred orientation. By the aid of equation (1), one finds that the intensity ratio should be

$$\frac{I(H)}{I(h)} = \kappa = \kappa_p \left(\cos^2 \alpha + \frac{\sin^2 \alpha}{r^3}\right)^{3/2}, \quad (13)$$

where α is the angle between vectors $\mathbf{H}$ and $\mathbf{h}$ and κ_p is the intensity ratio for a random powder, which can be routinely

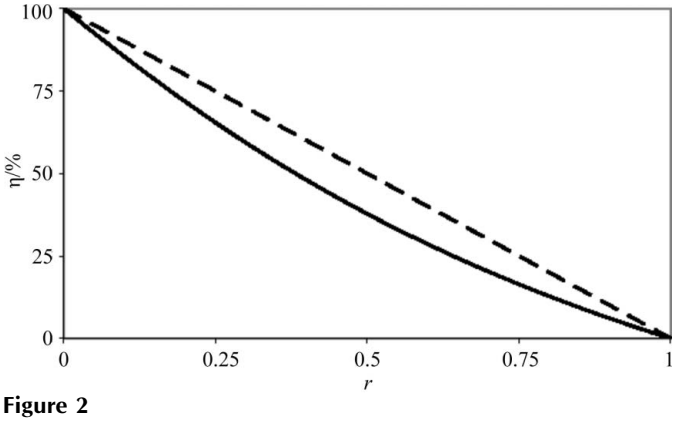

Figure 2
The degree of preferred orientation $\eta(r)$ as a function of the March parameter r, according to equation (12) (solid line). The linear dependence $\eta = 100\%(1 - r)$ is given for comparison.

calculated or taken from the ICDD files. The March parameter r is restored from equation (13) as

$$r = \left[\frac{\sin^2\alpha}{(\kappa/\kappa_p)^{2/3} - \cos^2\alpha}\right]^{1/3} \quad (14)$$

and is then used to find the η value by means of equation (12). According to equation (14), in the case of rather weak preferred orientation ($\kappa \geq \kappa_p$), the accuracy of the r determination will be higher when choosing a second atomic plane **h** to be inclined by a small angle ($\cos\alpha \leq 1$) with respect to the plane **H**.

3.1. Preferred orientation in the nacre of mollusc shells

We have applied the measurement of diffraction intensity ratios to map the preferred orientation in the nacre layer of aragonitic bivalve shells of *Acanthocardia tuberculata*. In these shells, which grow to about 40 mm in size, the entire nacre layer is 200–300 μm thick and is built of aragonite tablets, each a few micrometres long and 200–600 nm thick (see Zolotoyabko & Quintana, 2002*b*). The aragonite tablets reveal well developed preferred orientation of the [001] type clearly visible in scanning electron microscopy cross sections. This means that the aragonite crystals in the nacre layer grow with the *c* axis of the orthorhombic unit cell oriented preferentially along the normal to the inner surface of the shell (adjacent to the mollusc mantle). Aragonite tablets have a disk-like shape which is suitable for application of the March–Dollase approach. More details of various microstructures in mollusc shells are given by Chateigner *et al.* (2000) and Pokroy & Zolotoyabko (2003). In the case of a crossed lamellar microstructure, the degree of preferred orientation is not very high (see *e.g.* Pokroy & Zolotoyabko, 2003) and the texture may be refined together with structural parameters using the Rietveld refinement procedure (see *e.g.* Ouhenia *et al.*, 2008). In a well developed nacre layer, the degree of preferred orientation may be much higher (see *e.g.* Zolotoyabko & Quintana, 2002*a*) and, as we show below, the texture can be successfully characterized by measuring the intensity ratios of two diffraction lines.

X-ray diffraction measurements were carried out on the 5BMD beamline of the Advanced Photon Source (APS) at Argonne National Laboratory at an X-ray energy of 10 keV (for details, see Zolotoyabko & Quintana, 2002*a*). The $\theta/2\theta$ scans were taken from the inner (shiny) surfaces of nearly flat rectangular shell pieces, a few millimetres in size, which were cut from a mature shell using a diamond saw. The incident beam was restricted by slits to 1 mm vertically and 3 mm horizontally. A typical $\theta/2\theta$ scan is plotted on a logarithmic scale in Fig. 3 and shows a very strong preferred orientation of the [001] type, which is revealed as a greatly enhanced diffraction intensity originating from the (00*l*) reflections. Other diffraction lines are strongly suppressed. For example, the diffraction intensity ratio for the (002) and (012) atomic planes (having a small enough angle between them, $\alpha = 19.2^\circ$) is only $\kappa_p = 0.042$ for random aragonite powder. Owing to the high degree of preferred orientation, the intensity ratio $\kappa = I(002)/I(012)$ measured in the nacre layer is greatly increased and in some shells exceeds $\kappa = 100$. This is a clear case for applying the algorithm expressed by equations (13) and (14).

Using the intensity ratios $\kappa = I(002)/I(012)$ measured in different samples and applying equations (14) and (12), the η values for each sample were extracted. Since the investigated samples were taken from different locations over the entire shell, putting the obtained η values all together on the map yields the spatial distribution of the degree of preferred orientation across the inner surface of the shell. The resulting data are presented in the form of a 35-'pixel' map in Fig. 4. We note the rather large range of the measured η values, confined between 32 and 80%. The minimum $\eta = 32\%$ was found at $x = 25$, $y = 5$, near the shell apex, where the oldest shell material is concentrated. At the shell's rim, $y = 25$, where the youngest nacre layer is deposited, the η values are much higher, reaching the maximum $\eta = 80\%$ in a position located at $x = 20$, $y = 25$.

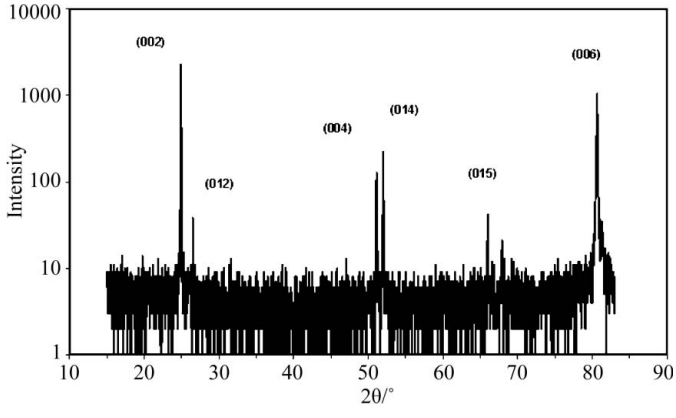

Figure 3
Diffraction data taken from one of the shells at 10 keV, showing the strong preferred orientation of the [001] type.

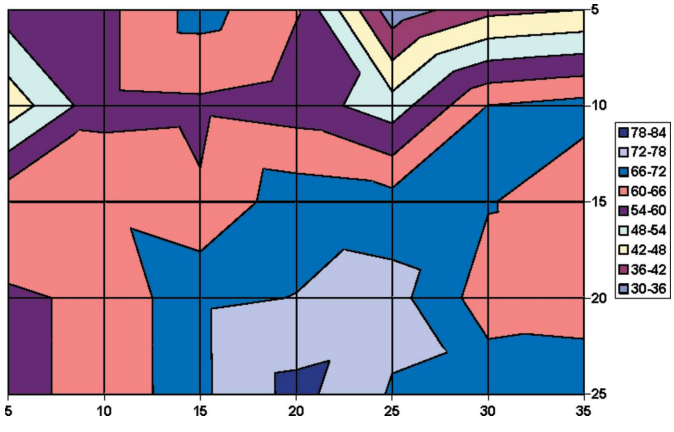

Figure 4
A map of the degree of preferred orientation η, showing the distribution of η values across the inner surface of the shell. Horizontal and vertical dimensions on the map are given in millimetres.

3.2. GaN growth on Si substrates

Our second example is taken from the field of artificial crystal growth, namely epitaxial growth of GaN films on [111]-oriented Si substrates by the metal–organic chemical vapour deposition technique. As shown by Zamir *et al.* (2000), in this case a buffer layer of AlN should be used in order to enhance the nucleation rate of GaN. The critical parameters for the successful growth of GaN on Si are the temperature T and the duration t of the growth of the buffer layer. To find the optimized growth conditions, we used laboratory X-ray diffraction measurements carried out using a Philips X-Pert system. Specifically, we performed $\theta/2\theta$ scans in the angular range that included the (002) (basal plane of the wurtzite-type GaN structure) and (102) GaN reflections. The latter is visible in diffraction scans with no overlap with the strong (002) reflection. The angle between the (001) and (102) atomic planes is $\alpha = 43.2^\circ$ and the intensity ratio for random powder is $\kappa_p = I(002)/I(102) = 0.83$. In the case of epitaxial GaN growth on [111]-oriented Si, the basal plane of GaN becomes the plane of preferred orientation and the intensity ratio $\kappa = I(002)/I(102)$ is greatly increased. We have used this fact to explain qualitatively the main features of the effect of the buffer layer on GaN growth (Zamir *et al.*, 2000). Here, we quantitatively describe the degree of preferred orientation in this system, applying equations (14) and (12) to the previously obtained X-ray diffraction ratios κ.

The effect of the buffer layer growth temperature on the quality of the GaN films is shown in Fig. 5. At low temperatures, $T \simeq 700$ K, the grown films are poor quality, characterized by a rather low degree of preferred orientation of less than 50%. The η values increase rapidly with temperature up to $\eta = 89\%$ at T $\simeq 760$ K. After that, the degree of preferred orientation increases very slowly with temperature, reaching the remarkable maximum value of $\eta = 90\%$ at $T \simeq 1100$ K. The change in growth mode at 760 K is explained in a paper by Zamir *et al.* (2000) in terms of the characteristics of AlN crystallites, which are governed by the interplay between nucleation and growth processes in the AlN layer.

Another important parameter is the growth duration t of the buffer layer. The degree of preferred orientation achieved in a GaN film at $T = 768$ K, as a function of growth duration t, is plotted in Fig. 6. At short durations of less than 3 min, and rather long durations of more than 6 min, the quality of the GaN films is very poor, revealing an extremely low degree of preferred orientation, $\eta \simeq 20\%$. The maximum preferred orientation, exceeding 86%, is achieved at $t = 5$ min. The existence of an optimum growth duration of the buffer layer is explained by Zamir *et al.* (2000) as the result of competition between crystal growth and self-annealing processes.

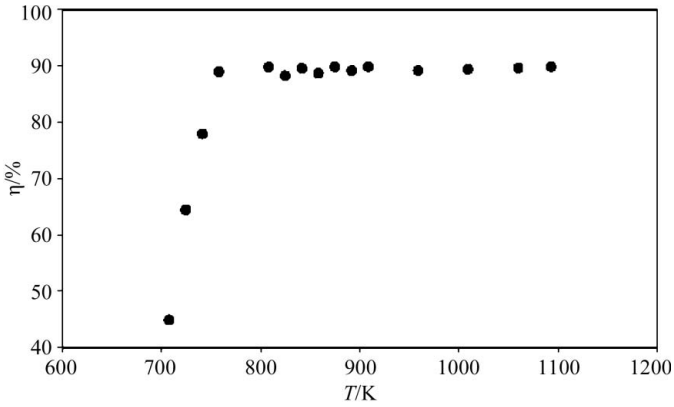

Figure 5
The degree of preferred orientation η in a GaN film, plotted as a function of the growth temperature of the AlN buffer layer.

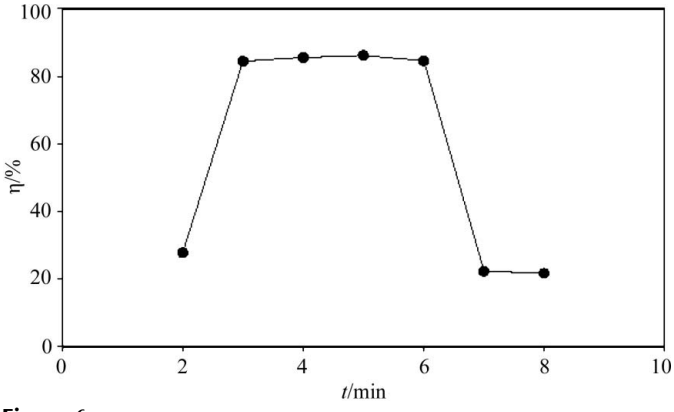

Figure 6
The degree of preferred orientation η in a GaN film, plotted as a function of the duration of the AlN buffer layer growth.

4. Conclusions

Working examples show that the procedure developed here provides valuable information on the degree of preferred orientation in different systems. It can be used to characterize material modifications under growth and processing. We stress that we are able to characterize the investigated systems quantitatively, *i.e.* to determine the proportion (in percent) of 'well organized' crystallites and to follow its modification as a function of various parameters. This is achieved using the newly developed equation (12), which connects the degree of preferred orientation to a single March parameter. The latter can be extracted from diffraction measurements, using Rietveld refinement of a whole diffraction pattern if the preferred orientation is rather weak, or by measuring the intensity ratios of two appropriately selected diffraction lines in cases where the preferred orientation is pronounced.

Experimental data relating to mollusc shells were collected at Sector 5 of the APS, which is run by the DuPont–Northwestern–Dow Collaborative Access Team (DND-CAT). The help of J. P. Quintana and B. Pokroy is gratefully acknowledged. Raw diffraction data from GaN films were kindly provided by S. Zamir and his contribution is highly appreciated. This work was partially supported by the Technion Fund for Promotion of Research.

References

Adams, B. L., Wright, S. I. & Kunze, K. (1993). *Metall. Trans. A*, **24**, 819–831.

Ahtee, M., Nurmela, M., Suortti, P. & Järvinen, M. (1989). *J. Appl. Cryst.* **22**, 261–268.

Bunge, H. J. (1982). *Texture Analysis in Materials Science: Mathematical Methods.* London: Butterworth.

Bunge, H. J. & Haessner, F. (1968). *J. Appl. Phys.* **39**, 5503–5514.

Čapková, P., Peschar, R. & Schenk, H. (1993). *J. Appl. Cryst.* **26**, 449–452.

Chateigner, D., Hedegaard, C. & Wenk, H.-R. (2000). *J. Struct. Geol.* **22**, 1723–1735.

Deyu, L., O'Connor, B., Roach, G. I. D. & Cornell, J. B. (1990). *Powder Diffr.* **5**, 79–85.

Dollase, W. A. (1986). *J. Appl. Cryst.* **19**, 267–272.

Howard, C. J. & Kisi, E. H. (2000). *J. Appl. Cryst.* **33**, 1434–1435.

Järvinen, M. (1993). *J. Appl. Cryst.* **26**, 525–531.

Kurtz, D. S., Kozaczek, K. J. & Morgan, P. R. (2001). US Patent No. 6301330B1.

Larson, A. C. & Von Dreele, R. B. (1986). *GSAS*. Report LAUR 86-748. Los Alamos National Laboratory, New Mexico, USA.

Leventouri, T. (1997). *Physica C*, **277**, 82–86.

Lutterotti, L., Matthies, S., Wenk, H. R., Schultz, A. S. & Richardson, J. W. (1997). *J. Appl. Phys.* **81**, 594–600.

March, A. (1932). *Z. Kristallogr.* **81**, 285–297.

Matthies, S., Lutteroti, L. & Wenk, H. R. (1997). *J. Appl. Cryst.* **30**, 31–42.

Matthies, S. & Vinel, G. W. (1982). *Phys. Status Solidi B*, **112**, K111–114.

Ouhenia, S., Chateigner, D., Belkhir, M. A. & Guilmeau, E. (2008). *J. Struct. Biol.* **163**, 175–184.

Pokroy, B. & Zolotoyabko, E. (2003). *J. Mater. Chem.* **13**, 682–688.

Popa, N. C. (1992). *J. Appl. Cryst.* **25**, 611–616.

Poulsen, H. F. (2004). *Three-Dimensional X-ray Diffraction Microscopy*, Springer Tracts in Modern Physics, Vol. 205. Berlin: Springer-Verlag.

Roe, R. J. (1965). *J. Appl. Phys.* **36**, 2024–2031.

Sitepu, H., O'Connor, B. H. & Li, D. (2005). *J. Appl. Cryst.* **38**, 158–167.

Sitepu, H., Prask, H. J. & Vaudin, M. D. (2001). *Adv. X-ray Anal.* **44**, 241–246.

Smith, K. L. & Ortega, R. B. (1993). *Adv. X-ray Anal.* **36**, 641–647.

Von Dreele, R. B. (1997). *J. Appl. Cryst.* **30**, 517–525.

Young, R. A. (1993). Editor. *The Rietveld Method.* Oxford University Press.

Zamir, S., Meyler, B., Zolotoyabko, E. & Salzman, J. (2000). *J. Cryst. Growth*, **218**, 181–190.

Zolotoyabko, E. & Quintana, J. P. (2002*a*). *Rev. Sci. Instrum.* **73**, 1663–1667.

Zolotoyabko, E. & Quintana, J. P. (2002*b*). *J. Appl. Cryst.* **35**, 594–599.